

Filled skutterudite antimonides: Electron crystals and phonon glasses

B. C. Sales, D. Mandrus, B. C. Chakoumakos, V. Keppens, and J. R. Thompson

Solid State Division, Oak Ridge National Laboratory, Oak Ridge, Tennessee 37831

(Received 19 May 1997; revised manuscript received 5 August 1997)

Crystallographic data, electrical and thermal transport measurements, and magnetic susceptibility values are reported for several compounds and alloys with the filled skutterudite structure, $R_{1-y}Fe_{4-x}Co_xSb_{12}$ ($R = La, Ce, \text{ or } Th; 0 < y < 1; x = 0, 1$). Room-temperature velocity of sound data is also reported. These materials are of interest because of their potential in thermoelectric power generation and refrigeration applications. The transport properties of both filled and unfilled skutterudite compounds are analyzed using standard semiconductor transport models. Filled skutterudite antimonides appear to be a good approximation of an idealized solid with the good electrical transport properties of a crystal but the poor heat conduction characteristics of a glass. The incoherent rattling of the weakly bound rare-earth atoms in these materials lowers the thermal conductivity at room temperature to values comparable to that of vitreous silica. Relative to the analogous unfilled compounds, the filled skutterudites exhibit larger effective masses and smaller mobilities. Good overall electrical transport is maintained, however, as evidenced by values for the figure of merit (ZT) greater than 1 at elevated temperatures (700–1000 K). Above room temperature, there is very little difference in the electrical and thermal transport behavior between the La and Ce filled compounds. The effects of the hybridization caused by the proximity of the Ce $4f$ level to the Fermi energy, however, are evident at temperatures below 300 K. [S0163-1829(97)02947-0]

I. INTRODUCTION

One of the more interesting ideas in the area of thermoelectric materials research is the concept of designing a solid that conducts heat like a glass but maintains the good electrical properties associated with crystals. The essence of the idea, as first proposed by Slack,¹ is to synthesize semiconducting compounds in which one of the atoms (or molecules) is weakly bound in an oversized atomic cage. Such an atom will undergo large local anharmonic vibrations, somewhat independent of the other atoms in the crystal, and hence will be referred to as a ‘‘rattler.’’ In insulating crystals localized rattlers (or Einstein oscillators) can in some cases dramatically lower the thermal conductivity to values comparable to the heat conducted by a glass with the same composition. The concentration, mass fraction, and frequency of the rattlers determine how much the thermal conductivity is lowered in a particular temperature range. Slack,² as well as Cahill and Pohl³ have proposed that the thermal conductivity of a crystal cannot be less than a minimum value, $\kappa_{\min} \cdot \kappa_{\min}$ is attained when the mean free path of the heat-carrying phonons becomes the order of the phonon wavelength and corresponds to the thermal conductivity of an amorphous solid with the same chemical composition.

While it is clear that rattlers should lower the lattice portion of the thermal conductivity, it is not obvious that good electronic transport can be maintained in such a material. Good electronic transport is defined to mean that which results in a material with a high value for the thermoelectric figure of merit, ZT , where

$$ZT = TS^2 / \kappa \rho. \quad (1)$$

S is the Seebeck coefficient (or thermopower), ρ is the electrical resistivity, T is the absolute temperature, and κ is the

total thermal conductivity. The total thermal conductivity is the sum of the heat conducted by the lattice, κ_L , and the heat transported by the electrical carriers κ_e . Finding more efficient thermoelectric materials for either refrigeration or power generation applications corresponds to finding materials with higher values of ZT .

The word skutterudite is derived from a town in Norway where minerals with this structure, such as $CoAs_3$, were first discovered. Compounds with the filled skutterudite structure were discovered by Jeitschko and Braun⁴ in 1977 and have the general formula of RM_4X_{12} , where X was P, As, or Sb; M was Fe, Ru, or Os; and R was La, Ce, Pr, Nd, or Eu.^{5–7} These compounds are body-centered cubic with 34 atoms in the conventional unit cell and space group $IM3$ (Fig. 1). (The primitive unit cell, which is sometimes used in theoretical estimates of the thermal conductivity, has only 17 atoms.⁸) This structure can be described as consisting of square planar rings of four pnictogen atoms (X) with the rings oriented along either the (100), (010), or (001) crystallographic directions. The metal (M) atoms form a simple cubic sublattice and the R atoms are positioned in the two remaining ‘‘holes’’ in the unit cell. X-ray^{4–7} and neutron structure refinements indicate that for many of the compounds the R atoms (such as La or Ce) tend to exhibit exceptionally large thermal parameters corresponding to the rattling of these atoms in an oversized atomic cage. As shown below, this rattling dramatically reduces the thermal conductivity of these filled skutterudite compounds. When the R atoms are absent from the structure, the basic skutterudite structure is formed.

Since the original papers of Jeitschko and Braun, many other variations of materials with this structure have been synthesized.^{9–16} Because these compounds are difficult to synthesize in pure form, the solid-state properties of most of these materials are unknown. Those compounds that have been successfully investigated, however, include several

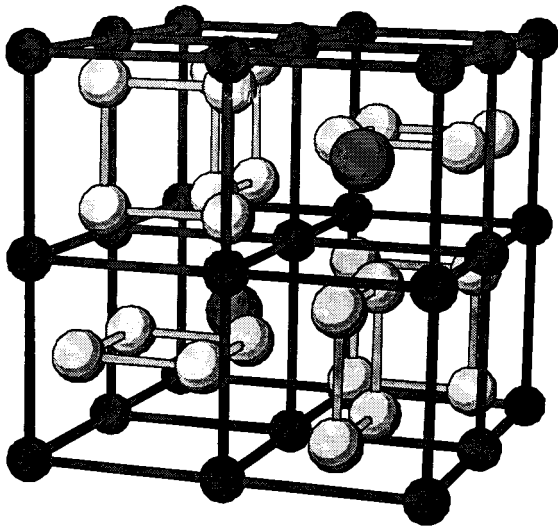


FIG. 1. Illustration of the filled skutterudite structure. For $\text{LaFe}_3\text{CoSb}_{12}$, the two large spheres represent the La atoms, the small dark gray spheres represent the Fe or Co atoms, and the light gray spheres represent Sb atoms. Note the four-membered Sb rings and the large “cage” in which the La resides. This illustration corresponds to the conventional unit cell shifted by the fractional coordinates $\frac{1}{4}, \frac{1}{4}, \frac{1}{4}$.

superconductors,^{10,14} a heavy-fermion metal,¹¹ Kondo-like narrow-gap semiconductors,¹² ferromagnets^{12,13} and, in the present case, narrow-gap semiconductors with moderate mobilities. Although our original motivation for the synthesis of these materials was to investigate the thermoelectric properties of so-called Kondo-insulators, reports on the thermoelectric properties of binary skutterudite compounds such as IrSb_3 , RhSb_3 , and CoSb_3 (Refs. 8 and 17–19) shifted our focus to more traditional narrow-gap semiconductors with the filled skutterudite structure. The binary skutterudite antimonides exhibit excellent electrical transport properties, including some of the highest values for hole mobility ever reported for a semiconductor.¹⁸ Unfortunately, the thermal conductivities of these binary antimonides are too large for thermoelectric applications.¹⁹

Ternary semiconductors with the filled skutterudite structure provide another degree of freedom in optimizing thermoelectric properties relative to their binary counterparts. Our previous work²⁰ showed that some of these materials had large values of ZT at elevated temperatures. The present article examines whether the filled skutterudite antimonides should be regarded as a realization of Slack’s electron-crystal phonon-glass concept.

II. EXPERIMENTAL METHODS

A. Synthesis

The synthesis of $R_{1-y}\text{Fe}_{4-x}\text{Co}_x\text{Sb}_{12}$ ($R = \text{La, Ce, Nd, Sm, Eu, or Th}$; $0 < y < 1$; $0 < x < 4$) alloys (this illustrates some of the alloys we have synthesized—only representative compositions are discussed in the present manuscript) is complicated by the peritectic decomposition of the solid phase at temperatures between 750 °C and 850 °C, the tendency of the rare-earth metal to only partially fill its crystallographic site,

the reactivity of rare-earth metals with most crucible materials, and the high vapor pressure of antimony at the optimum reaction temperatures (1000–1100 °C). A variety of synthesis approaches were investigated that involved the pre-reaction of two or more of the constituents (e.g., arc melting of the rare-earth and transition metals together). After a relatively extensive investigation of various synthesis methods, a simple and clean synthesis approach was developed.

A thin layer of carbon was deposited on the inside of a round-bottomed silica tube by the pyrolysis of acetone. Stoichiometric amounts of high purity rare earth metal pieces (99.99% electropolished bar from AMES research laboratory), Fe rod (99.9985% from Alfa Chemical Company), Co rod (99.998% from Alfa), and Sb shot (99.999% from Alfa) were loaded into the precarbonized tube. The tube was sealed under vacuum at a pressure of 10^{-3} Pa and transferred into a programmable furnace. The silica ampoule was heated to 600 °C at 2 °C/min, left at 600 °C for 3 h, and then slowly (0.5 °C/min) heated to 1050 °C and left for about 20 h. It is important to slowly heat the tube because of the highly exothermic reaction between the rare-earth elements (particularly Ce) and Sb. The silica ampoule containing the homogeneous molten liquid was removed from the furnace at temperature and quenched into a water bath. The same ampoule (containing the pre-reacted elements) was then placed in a furnace and annealed at 700 °C for 30 h to form the correct crystallographic phase. The completely reacted solid was removed from the silica tube and cleaned with a wire brush to remove small amounts of carbon from the surface. To form a completely dense polycrystalline solid, the reacted material was ball milled into a fine powder in an argon atmosphere, loaded into a graphite die, and hot pressed (3.5 GPa) in a helium atmosphere at 700 °C for 40 min. For transport measurements rectangular solids (e.g., $6 \times 6 \times 12 \text{ mm}^3$ or $7 \times 2 \times 18 \text{ mm}^3$) were cut from the hot-pressed material using a low speed diamond saw. Each sample was characterized using x-ray-diffraction, electrical resistivity, Hall, Seebeck, and thermal-conductivity measurements. Metallographic, energy dispersive x-ray (EDX) and magnetic measurements were performed on selected samples. A typical x-ray pattern from a filled skutterudite antimonide is shown in Fig. 2. Most samples had less than 3 vol % of an impurity phase such as FeSb_2 or RSb_2 , were better than 95% of the theoretical x-ray density, and had polycrystalline grains in the 5–50 micrometer range.

Single crystals of $\text{La}_{1-y}\text{Fe}_{4-x}\text{Co}_x\text{Sb}_{12}$ were grown using the Bridgmann technique with an excess of antimony (Sb_{20}). In a real-time neutron-diffraction camera, the bottom of the boule appeared to be a large single crystal approximately $4 \times 1 \times 1 \text{ cm}^3$. Upon closer examination, however, the bottom portion of the “crystal” was Co rich and the top portion was Fe rich relative to the starting composition. There were also polycrystalline Sb inclusions throughout the crystal. Although the material was not suitable for transport measurements, small single-crystal cubes measuring $2 \times 2 \times 2 \text{ mm}^3$ were found to be excellent for crystallographic investigations of the structure as a function of temperature. For the purposes of comparison, polycrystalline samples of the unfilled skutterudite, CoSb_3 , were synthesized using the same method (described above) used to prepare the filled skutterudites.

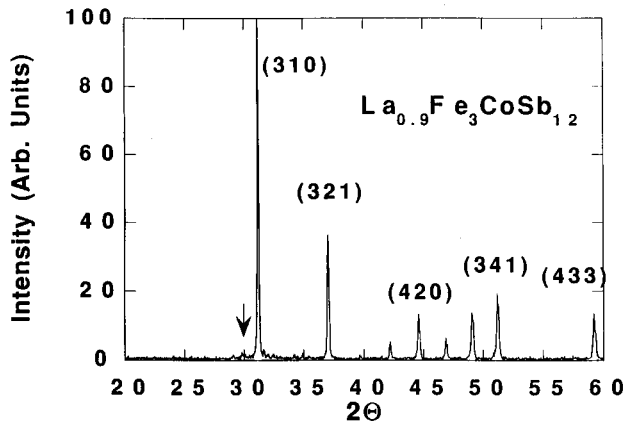


FIG. 2. Typical powder x-ray-diffraction pattern from a filled skutterudite antimonide. The Miller indices for several of the peaks are noted. The arrow denotes the largest impurity peak observed in this sample.

B. Measurements

Powder x-ray-diffraction measurements were made using $\text{Cu } K\alpha$ radiation and a commercial SCINTAG diffractometer equipped with a nitrogen-cooled Ge detector. The single-crystal neutron-diffraction experiments were conducted at ORNL's High Flux Isotope Reactor using a four-circle neutron diffractometer and a liquid-helium system. Chemical composition information was obtained directly using a Princeton Gamma Tech energy dispersive x-ray system and an International Scientific Instruments scanning electron microscope. Metallographic investigations were performed on polished surfaces using standard optical microscopy techniques. Magnetic susceptibility measurements were made from 4–300 K using a commercial SQUID magnetometer from Quantum Design. Room-temperature velocity of sound measurements were made on polycrystalline samples using a commercial resonant ultrasound system from Quatrosomics.²¹

Electrical and thermal transport data from 10–300 K were obtained using a closed cycle helium refrigerator. The sample was suspended from a copper cold finger using EPO-TEK H20E silver epoxy. A small RuO_2 chip resistor (51 Ω) was attached to the other end of the sample using a thermally conducting but insulating epoxy from EPO-TEK (930-4). Electrical connections to the heater were made with Woods metal and 0.0075-cm chromel wires. Small temperature differences (1–3 K) across the sample were measured using two 0.0125-cm chromel-constantin thermocouples attached to the sample using silver paint. For Seebeck and resistivity measurements, four 0.0075-cm copper wires were attached to the sample with silver paint. The sample and wires were enclosed in a copper can that was thermally attached to the cold finger. The copper can was at approximately the same temperature as the cold end of the sample. Using this arrangement radiation losses were kept to a minimum. For samples with values for thermal conductivity of 100 mW/cm K and above, the radiation and conduction losses were small enough to be neglected regardless of the geometry of the sample. However, many of the filled skutterudites had thermal conductivities (at room temperature) in the 15–30 mW/cm K range. To obtain reliable thermal conductivity

values for these materials, all of the copper leads were removed from the sample and the samples were cut into a specific shape ($6 \times 6 \times 12 \text{ mm}^3$) which had a relatively large ratio of the cross-sectional area to length. It was found that this procedure yielded the correct thermal-conductivity values for a vitreous SiO_2 standard over the entire 10–300 K temperature interval. If a small bar-shaped sample was used instead, the thermal conductivity of the lattice showed pronounced upward curvature in the 200–300 K temperature range—a feature characteristic of problems with radiation losses. Hall measurements at room and nitrogen temperatures were made on 0.025-cm-thick slabs using the van der Pauw technique with an excitation current of 100 mA. Assuming a single carrier band and a scattering factor of 1, the carrier density was calculated from the Hall coefficient. Because of the high carrier concentrations (10^{19} – $5 \times 10^{21} \text{ cm}^{-3}$) observed in most of the samples, measurements were performed with the Hall probe immersed in methanol (295 K) or liquid nitrogen (77 K) to minimize thermal voltages. The methods used to measure the thermal conductivity, Seebeck coefficient, and resistivity of the filled skutterudites at elevated temperatures (300–800 K) have been described previously.²⁰

III. RESULTS AND DISCUSSION

A. Evidence of “rattling”

The most direct evidence of rattling comes from structure refinements obtained using either x-ray^{4–7,9} or neutron scattering on single crystals. Unusually large rare-earth atomic displacement parameters (formerly called thermal parameters) are clear indications of the “rattling” of the rare-earth ion in an oversized atomic cage. For example, Braun and Jeitschko⁵ noted that in the $\text{LaFe}_4\text{Sb}_{12}$ compound that the “lanthanum atoms seem to rattle.” For single phase polycrystalline or single-crystal samples, an atomic displacement parameter (ADP) can be obtained for each distinct atom in the crystal structure. In the simplest situation this parameter measures the mean-square displacement of the atom about its equilibrium position and hence is a direct measure of the rattling. To insure that the ADP parameter does measure the rattling (as opposed to reflecting systematic errors generated during the refinement), the occupation of the various crystallographic sites are treated as adjustable parameters during the data refinement. Figure 3 shows the ADP parameters for La, Fe, Co, and Sb obtained from a single crystal with the refined composition $\text{La}_{0.75}\text{Fe}_3\text{CoSb}_{12}$. The ADP values for Fe, Co, and Sb are typical for these elements in compounds with similar coordination numbers. The ADP values for La, however, are anomalously large, particularly near room temperature. These values indicate that the La is poorly bonded in the structure and “rattles” about its equilibrium position with an average amplitude of 0.015 nm. A more complete discussion of the La ADP parameter will be presented elsewhere.²²

A preliminary study has been made of the characteristic energies or frequencies associated with the rattling.²³ Elastic constant measurements indicate that the low-temperature behavior of the filled skutterudite $\text{La}_{0.75}\text{Fe}_3\text{CoSb}_{12}$ is anomalous relative to its unfilled analog, CoSb_3 . The $\text{La}_{0.75}\text{Fe}_3\text{CoSb}_{12}$ data could be modeled using two two-level

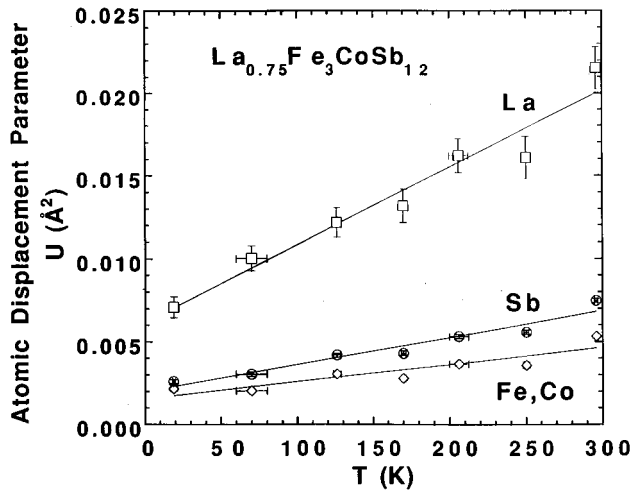


FIG. 3. Refined atomic displacement parameters obtained on a single crystal of $\text{La}_{0.75}\text{Fe}_3\text{CoSb}_{12}$ using a four-circle neutron diffractometer. The crystal was approximately 2 mm on a side. The large value of the atomic displacement parameter for the La atom is indicative of the rattling of the La atom in an oversized atomic cage.

systems with level spacings of 50 and 200 K. Low-temperature heat-capacity measurements on a similar filled skutterudite ($\text{La}_{0.9}\text{Fe}_3\text{CoSb}_{12}$) sample also indicated that the thermodynamics of these materials are unusual. An analysis of the heat-capacity data from 0.5 to 45 K required two Einstein oscillators with characteristic temperatures of 70 and 157 K to model the data. Localized vibrations should also be evident as narrow peaks in the phonon density of states. Preliminary inelastic neutron-scattering measurements on a 30-g polycrystalline sample of $\text{La}_{0.9}\text{Fe}_3\text{CoSb}_{12}$ show two peaks in the phonon density of states at 100 and 240 K. Although it is tempting to associate these peaks with the anomalies found in the elastic constant and heat-capacity measurements, more data is required from the unfilled skutterudite (CoSb_3) before assessing the self-consistency of these measurements. Further heat capacity and inelastic neutron-scattering measurements are in progress.

B. Rattling and thermal conductivity

Shown in Fig. 4 is a comparison between the lattice thermal conductivity of CoSb_3 and two filled skutterudites $\text{CeFe}_4\text{Sb}_{12}$ and $\text{La}_{0.75}\text{Th}_{0.2}\text{Fe}_3\text{CoSb}_{12}$. The data for these two filled skutterudites brackets the values we have found for this family of materials. At room temperature, samples with a rattler (i.e., filled) have values for the thermal conductivity 6–8 times lower than the unfilled ceramic CoSb_3 .

The Wiedemann-Franz law with a value for the Lorenz number of $2 \times 10^{-8} \text{ V}^2/\text{K}^2$ has been used to estimate the electronic contribution to the thermal conductivity. This value is a reasonable approximation for a heavily doped semiconductor²⁶ The classical value of Lorenz number of $2.44 \times 10^{-8} \text{ V}^2/\text{K}^2$ is appropriate for a degenerate electron gas (i.e., a metal). If, however, the classical value is used to estimate the electronic portion of the thermal conductivity, the lattice contribution at room temperature to the thermal conductivity of the filled skutterudites shown in Fig. 5 is reduced by 1–2 mW/cm K.

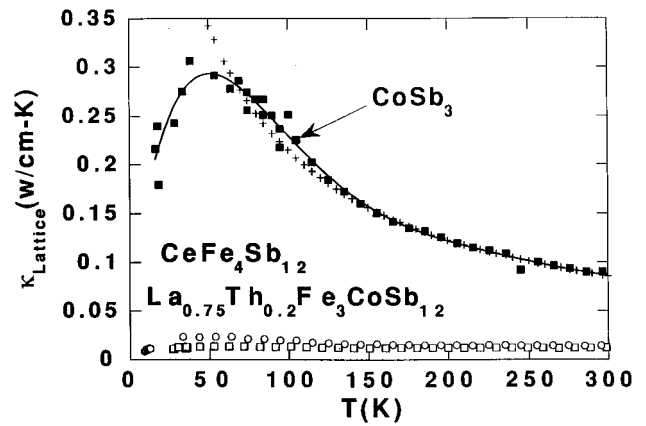


FIG. 4. Lattice component of the thermal conductivity of CoSb_3 and two filled skutterudites $\text{CeFe}_4\text{Sb}_{12}$ (open circles) and $\text{La}_{0.75}\text{Th}_{0.2}\text{Fe}_3\text{CoSb}_{12}$ (open squares). The data for these two filled skutterudites bracket the thermal conductivity values we have found for this family of materials. The CoSb_3 data above 60 K are well described by $1/(A+BT)$ (crosses) with $A=1.176 \text{ cm K/W}$ and $B=0.0348 \text{ cm/W}$. The solid line through the CoSb_3 data is a guide to the eye.

Most discussions²⁴ of the lattice thermal conductivity use an expression adapted from the kinetic theory of gases: $\kappa_L = 1/3 C_v v_s d$, where C_v is the heat capacity per unit volume, v_s is an average velocity of sound, and d is the mean free path of the heat-carrying phonons. In crystalline materials at high temperatures C_v and v_s are approximately constant, and the mean free path, d , decreases as $1/T$ as the number of phonons increase. At lower temperatures d is often dominated by scattering from static defects and approaches a constant. Therefore, at temperatures above where the heat capacity is rapidly changing the lattice thermal conductivity is approximately given $1/(A+BT)$, where A and B are constants. This simple expression accurately describes the CoSb_3 data above 60 K (Fig. 4) with $A=1.176 \text{ cm KW}$ and $B=0.0348 \text{ cm/W}$. The lattice thermal conductivity of CoSb_3 is typical of a crystalline material.

C. How glasslike is the thermal conductivity?

The lattice thermal conductivities from representative filled skutterudite alloys are shown in Fig. 5. The thermal conductivities of these compounds are clearly quite low but are they glasslike? The simplest estimate of the minimum thermal conductivity (κ_{\min}) of these materials is obtained with $\kappa_L = 1/3 C_v v_s d$, by setting d equal to an interatomic spacing (about 0.3 nm) and using the Dulong and Petit value for C_v . The transverse, v_t , and longitudinal, v_l , velocity of sound has been measured on CoSb_3 and two filled skutterudites using resonant ultrasound spectroscopy and are given in Table I. Using an average value for v_s of $(2v_t + v_l)/3$ yields a value for κ_{\min} of 6 mW/cm K. The measured value (about 15 mW/cm K) is a little more than twice the minimum value and corresponds to a mean free path of 0.75 nm. The nearest-neighbor separation between the rare-earth rattlers in the crystal is 0.8 nm.

In a real glass, such as vitreous SiO_2 , (Fig. 5) the thermal conductivity slowly decreases from room temperature to 10

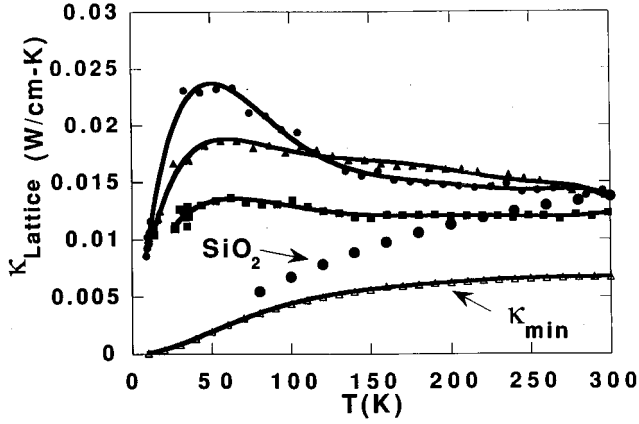


FIG. 5. Lattice component of the thermal conductivity of three filled skutterudites: $\text{CeFe}_4\text{Sb}_{12}$ (circles), $\text{Ce}_{0.75}\text{Th}_{0.2}\text{Fe}_3\text{CoSb}_{12}$ (triangles), and $\text{La}_{0.75}\text{Th}_{0.2}\text{Fe}_3\text{CoSb}_{12}$ (squares). The values for κ_{\min} were calculated using the velocity of sound data shown in Table I and Eq. (17) from Ref. 3. Also shown for comparison are the thermal conductivity values for vitreous silica (large circles) (Ref. 3).

K. A useful phenomenological expression was proposed by Cahill, Watson, and Pohl³ to describe the thermal conductivity of amorphous solids above 10 K. The only input to this model is the transverse and longitudinal velocities of sound and the number of atoms per unit volume. For a variety of amorphous solids they found this expression to be in good agreement with the measured data. Furthermore, based on a large amount of thermal-conductivity data from highly disordered crystals, Cahill, Watson, and Pohl³ proposed that this phenomenological expression represented κ_{\min} for a disordered crystal. κ_{\min} for the filled-skutterudite antimonides is shown in Fig. 5 and was calculated using Cahill's expression [Eq. (17), Ref. 3] and the velocity of sound data from Table I. The actual thermal conductivity data (Fig. 5) from the filled skutterudites (30–300 K) slowly increase or are roughly constant with decreasing temperature, unlike a true glass. Although the rattlers significantly lower the thermal conductivity of these compounds, the temperature dependence of κ_{Lattice} indicates that some characteristics of a crystalline solid remain.

D. Rattling and electrical transport

Although the thermal conductivity of the filled skutterudites is low, most of the interest is due to the ability of these materials to maintain relatively good electrical properties which results in large values for ZT . ZT versus T is shown in Fig. 6 for two nearly optimized filled skutterudite samples.

TABLE I. Velocity of sound data for polycrystalline skutterudites. The Debye temperature was calculated from the sound data.

Compound	Transverse sound velocity (m/s)	Longitudinal sound velocity (m/s)	Debye temperature (K)
CoSb_3	2788	4623	321
$\text{Ce}_{0.75}\text{Fe}_3\text{CoSb}_{12}$	2713	4559	312
$\text{La}_{0.75}\text{Fe}_3\text{CoSb}_{12}$	2661	4484	308

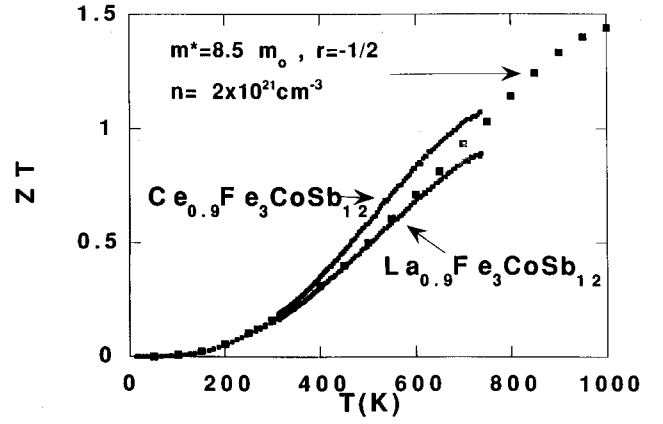


FIG. 6. ZT versus temperature for two nearly optimized filled skutterudites. A model calculation (see text) indicates that for these two compounds a maximum value of $ZT = 1.4$ is attained at 1000 K. The optimum carrier concentration, n , and the effective mass, m^* , are large in these materials.

For the Ce compound, ZT is greater than 1 at temperatures above 700 K. The model calculations, described below, indicate a maximum value for ZT of 1.4 at 1000 K. Recent measurements²⁵ at higher temperatures indicate that these large values for ZT may actually be attained. At temperatures much above 1000 K the compounds decompose.

The electrical transport in these materials was modeled using the Boltzmann equation, parabolic bands, and the assumption that the relaxation time was given by $\tau = \tau_0 E^r$. The energy E is measured from the edge of the valence band, τ_0 is a constant, and the scattering exponent r is used to parametrize the dominant scattering mechanism experienced by the electrons or holes. Typically a value of $r = -1/2$ is used for scattering by acoustic phonons, and $r = 3/2$ for scattering by ionized impurities. With these assumptions, the transport coefficients can be parametrized by the extrinsic carrier concentration, n , the effective mass of the band, m^* , τ_0 , and r . The transport coefficients²⁶ can then be expressed in terms of the integrals K_s :

$$\sigma = 1/\rho = e^2 K_0/T, \quad (2)$$

$$S = \pm (E_f/kT - K_1/K_0)/eT, \quad (3)$$

$$\kappa_e = (K_2 - K_1^2/K_0)/T^2, \quad (4)$$

where

$$K_s = (8\pi/3)(2/h^2)^{3/2}(m^*)^{1/2}T\tau_0(s+r+3/2) \times (k_B T)^{s+r+3/2} F_{s+r+1/2}, \quad (5)$$

and the Fermi-Dirac integrals F_n are given by

$$F_n(E_f/k_B T) = \int_0^\infty x^n f_0(x) dx, \quad (6)$$

with

$$x = E/k_B T, \quad \text{and} \quad f_0(x) = 1/[1 + e^{(x - E_f/k_B T)}]. \quad (7)$$

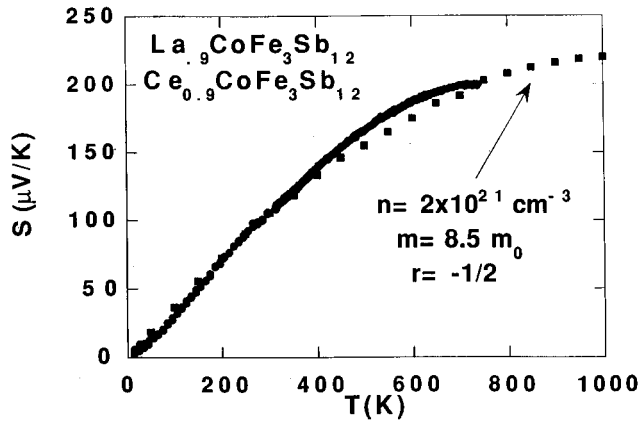


FIG. 7. Seebeck coefficient versus temperature for the two filled skutterudites shown in Fig. 6. The model calculation (solid squares) is in good agreement with the experimental data from 10–700 K.

These equations provide a crude model for the transport data. The temperature dependence of the mobility provides an estimate for r . Since for most of the filled skutterudite samples we investigated, the mobility, as determined from our Hall measurements, increased with decreasing temperature, a reasonable value for r is $-1/2$ (scattering dominated by acoustic phonons). The value of the Seebeck coefficient at a temperature where there are very few intrinsic carriers provides a value for the Fermi energy, E_f , since S only depends on $E_f/k_B T$ and r . We have estimated an energy gap of 0.4 ± 0.1 eV for filled skutterudite antimonides from high-temperature transport data on samples with low carrier concentrations.²⁰ (Note that the transport data shown in Fig. 8 are for heavily doped samples that yield the largest values for ZT . For these samples metallic behavior due to extrinsic doping is observed even at our highest measuring temperature of 800 K.) Therefore the value of S at room temperature should be dominated by extrinsic carriers and can be used to determine the Fermi energy. With the Fermi energy known, and using our Hall data to estimate the room-temperature carrier concentration, the effective mass can be determined. The measured value of the electrical resistivity at room temperature fixes τ_0 . Assuming that the extrinsic carrier concentration remains constant (saturation range), the temperature dependence of the Seebeck coefficient, the electrical resistivity, and the electronic contribution to the thermal conductivity then can be calculated using Eqs. (2)–(4). The expressions as shown can be easily modified to include another parabolic band that accounts for the generation of intrinsic carriers at temperatures comparable to the gap.

The measured and calculated Seebeck and resistivity data are compared in Figs. 7 and 8 for the same two skutterudite samples shown in Fig. 6. Considering that only the data at room temperature are used in computing the curves, the agreement between the model predictions and the measured data is quite good. The Seebeck data are well described by the one band model from 10–700 K. The general slope of the resistivity data for the La filled skutterudite is in fair agreement with the model over the entire temperature range. For the Ce compound, however, the resistivity data below 200 K are strongly affected by the proximity of the Ce 4*f* level to the Fermi energy. In other filled skutterudite materials such

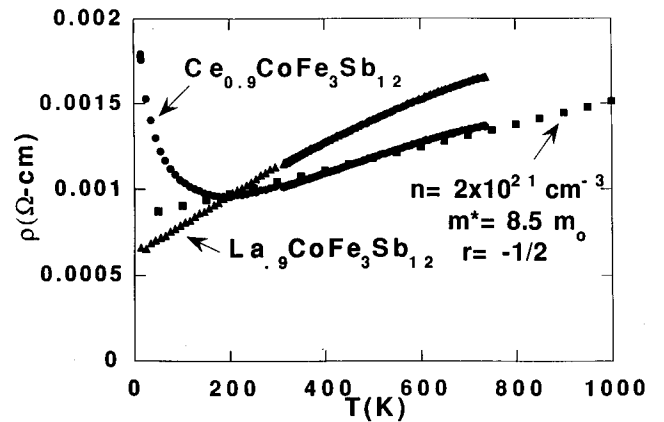


FIG. 8. Resistivity versus temperature for the two filled skutterudites shown in Fig. 6. The general slope of the resistivity data from the La filled skutterudite is in fair agreement with the model calculation (solid squares) over the entire temperature range. The Ce resistivity data below 200 K, however, are strongly affected by the proximity of the Ce 4*f* level to the Fermi energy.

as $\text{CeFe}_4\text{P}_{12}$ (Ref. 12) and $\text{CeRu}_4\text{P}_{12}$,^{16,27} the hybridization between the Ce and the pnictide bands actually causes a small gap to develop and the resistivity increases to values near $1000 \Omega \text{ cm}$ at 10 K.

Once r , m^* , and τ_0 have been determined for a particular carrier concentration, the carrier concentration can be changed in the calculation to assess how ZT varies with n . For moderate variations in n , this makes it possible to determine the optimum doping necessary to yield the maximum value for ZT without having to synthesize a large number of samples. Using this method it was determined that the alloys shown in Fig. 6 have close to the optimum doping of 2×10^{21} holes cm^3 necessary to maximize ZT . The maximum value of ZT at a particular temperature can be estimated using the same calculation. At room temperature the maximum value for ZT was found to be only 0.3. Using this method to extrapolate over large variations in carrier concentration is risky, however, since the mobility and m^* can change significantly with n .

Table II shows a comparison between the electronic transport parameters of the filled and unfilled skutterudites. Although the data shown in Table II were taken in our laboratory, the values given in the table are in good agreement with

TABLE II. Comparison of the electronic properties of polycrystalline unfilled and filled skutterudite antimonides using data taken in our laboratory.

Property	Filled	Unfilled
Energy gap from transport	$0.4 \text{ eV} \pm 0.1$	$0.4 \text{ eV} \pm 0.1$
Extrinsic carrier concentration (Typical)	10^{21} cm^{-3}	10^{17} cm^{-3}
Mobility (296 K)	$2-10 \text{ cm}^2/\text{V s}$	$1070 \text{ cm}^2/\text{V s}$
Effective mass	8	0.05

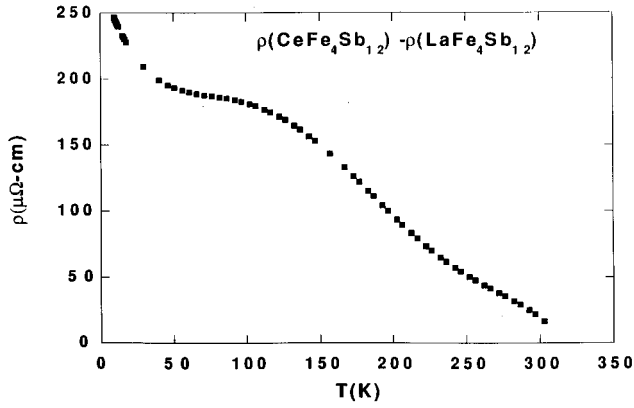


FIG. 9. Resistivity of $\text{CeFe}_4\text{Sb}_{12}$ minus the resistivity of $\text{LaFe}_4\text{Sb}_{12}$ versus temperature.

recent measurements reported in the literature.^{17,19,28} It is difficult to assess the extent to which the rattler degrades the electronic transport because of the large difference in carrier concentrations between the two materials (10^{21} cm^{-3} for the filled versus 10^{17} cm^{-3} for the unfilled). The larger carrier concentrations in the filled materials are due largely to the lack of complete filling of the rare-earth site. A 1% change in rare-earth concentration results in a formal change of the carrier concentration of about 10^{20} cm^{-3} . Alloys that contain 1 Co per formula unit, such as $\text{La}_y\text{Fe}_3\text{CoSb}_{12}$, can have values of y between about 0.9 and 0.7, depending on the exact synthesis conditions. This implies carrier concentrations in the range of $(1-3) \times 10^{21} \text{ cm}^{-3}$, as is observed. With increasing Co substitution the maximum filling of the rare-earth site decreases further^{20,28} but eventually n -type samples are obtained near Co substitutions of 2.5 per formula unit. Band-structure calculations²⁹ indicate that if all of the rare-earth sites could be filled in a $\text{LaFe}_3\text{CoSb}_{12}$ sample, better thermoelectric properties would result.

E. Effects of Ce on the transport and magnetic properties

As noted in the Introduction, one of the major reasons for the initial investigation of the filled skutterudites in our group was the unusual narrow-gap semiconductors such as $\text{CeFe}_4\text{P}_{12}$.¹² Although the Ce does not seem to play a significant role in the high-temperature thermoelectric properties of these materials, it clearly effects the low-temperature properties such as the electrical resistivity (Fig. 8). The compound $\text{CeFe}_4\text{Sb}_{12}$ is not an obvious semiconductor, and it has been proposed that this compound may be a heavy Fermion metal.¹¹ A rough idea of the effect of the Ce $4f$ electrons on the electrical transport in $\text{CeFe}_4\text{Sb}_{12}$ can be estimated by subtracting from the resistivity and Seebeck data of this compound the resistivity and Seebeck data of $\text{LaFe}_4\text{Sb}_{12}$. (In general, it is difficult to compare in detail the resistivity behavior from two polycrystalline compounds. For these two samples, however, the density and grain sizes were very close, as were the resistivity values at room temperature). These data are shown in Figs. 9 and 10 and illustrate the tendency of the Ce $4f$ level to hybridize and form a gap at low temperatures. The peak in the thermopower at 50 K is typical both in location and magnitude for Ce compounds

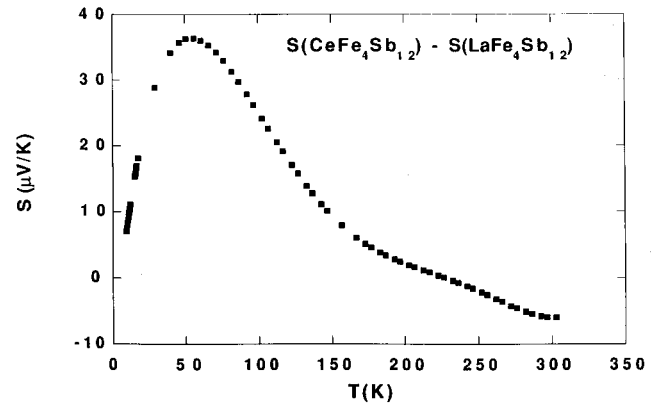


FIG. 10. Seebeck coefficient of $\text{CeFe}_4\text{Sb}_{12}$ minus the Seebeck coefficient of $\text{LaFe}_4\text{Sb}_{12}$ versus temperature.

with a $4f$ level close to the Fermi energy. Also note that near room temperature (and above) there is very little difference in behavior between the La and Ce compounds.

The magnetic behavior of $\text{CeFe}_4\text{Sb}_{12}$ and other isostructural rare-earth compounds has been reported previously.^{11,13,28} The previous analyses of the data from the Ce compounds, however, did not take into account the magnetic susceptibility due to the transition metals and the effects of crystalline electric fields on the magnetic response of the Ce ion. To determine the approximate valence and coupling among the Ce ions, susceptibility measurements were made on samples of $\text{La}_{0.9}\text{Fe}_3\text{CoSb}_{12}$ and $\text{Ce}_{0.9}\text{Fe}_3\text{CoSb}_{12}$ from 4–300 K. The susceptibility data from the La compound were paramagnetic and accurately described by $\chi = C/(T + \theta)$, with $C = 0.796 \text{ cm}^3 \text{ K/mol}$ and $\theta = 120.5 \text{ K}$ for temperatures between 5 and 300 K. Within the local-moment approximation the Curie constant corresponds to a magnetic moment of about $0.63 \mu_B$ per transition metal. The susceptibility of the La compound was treated as a correction and was subtracted from that of the Ce compound. The remaining susceptibility is presumably due to the magnetism associated with Ce. The correction from the La compound is about 30–35 % from 50 to 300 K decreasing to about 10% at 5 K.

The corrected inverse susceptibility for the $\text{Ce}_{0.9}\text{Fe}_3\text{CoSb}_{12}$ compound is shown in Fig. 11. The effects of crystalline electric fields on the magnetic susceptibility of Ce compounds are well known.³⁰ In a cubic environment the $J = \frac{5}{2}$ Hund's rule ground state of the Ce ion, which has a degeneracy of 6, is split into a doublet and a quartet.³¹ If, as a first approximation, the magnetic interactions among the Ce^{+3} ions are ignored, the susceptibility is given by

$$\chi = [C_{\text{free ion}}/T]F(T_{cf}/T), \quad (8)$$

where $C_{\text{free ion}} = N_A p^2 \mu_B^2 / 3K_B$, $p = 2.54$, T_{cf} is the splitting in K between the doublet and the quartet, $x = T_{cf}/T$, and

$$F(x) = [5/21 + (26/21)e^{-x} + (32/21x)(1 - e^{-x})]/(1 + 2e^{-x}). \quad (9)$$

The best fit to the data was obtained with the assumption that the doublet was lowest in energy and separated from the quartet by $350 \pm 50 \text{ K}$ and the effective moment was $2.9 \mu_B$

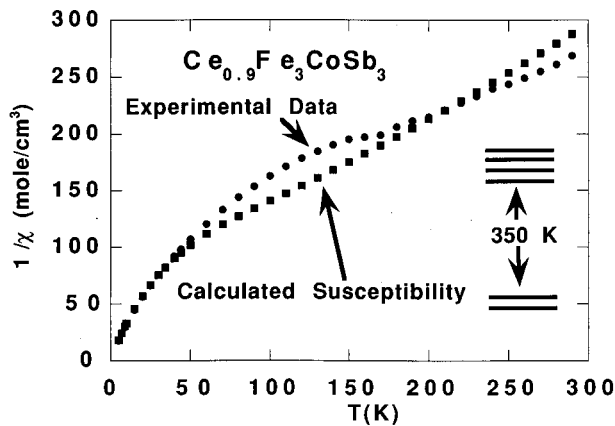


FIG. 11. Inverse magnetic susceptibility of $\text{Ce}_{0.9}\text{Fe}_3\text{CoSb}_{12}$ versus temperature. The susceptibility has been corrected for the transition-metal magnetism by subtracting the susceptibility of $\text{La}_{0.9}\text{Fe}_3\text{CoSb}_{12}$. An ionic model that includes the effects of a cubic crystalline electric field on the magnetic response of the Ce^{+3} ion is also shown. A splitting of 350 K between the ground-state doublet and the excited-state quartet was found to yield the best agreement between the model and the experimental data.

rather than the ionic value of $2.54\mu_B$. The larger effective moment could either be due to polarization of conduction electrons or to errors associated with correcting for the transition-metal magnetism. At low temperatures (below 15 K) the magnetism due to the Ce ions is dominant and the susceptibility follows a Curie law with an effective moment of $1.5\mu_B$. This is very close to the moment expected from the doublet of $1.4\mu_B$ [at low-temperatures $F(x)$ approaches $5/21$]. Although the agreement between this model and the experimental data is not perfect, it indicates that the Ce valence is close to 3 (3–3.1) over the entire temperature range. Even without any modeling, the fact that the susceptibility follows a Curie law of the expected magnitude at low temperatures indicates that the Ce valence is close to 3. (Ce compounds that undergo significant valence fluctuations exhibit a temperature-independent susceptibility at low temperatures.³²) This conclusion, however, is not in disagreement with the hypothesis that the Ce 4*f* level is close to the Fermi energy in these materials.

IV. SUMMARY AND CONCLUSIONS

The filled skutterudite antimonides appear to represent excellent examples of electron-crystal, phonon-glass materials.

The incoherent rattling of the loosely bound rare-earth atoms in these materials is inferred from the large values of the ADP parameter obtained in single-crystal structure refinements. This rattling lowers the thermal conductivity at room temperature to values within two to three times κ_{\min} . The estimated mean free path of the heat-carrying phonons at room temperature is 0.75 nm which agrees well with the nearest-neighbor separation of the rattlers, 0.8 nm. The temperature dependence of the thermal conductivity of these materials below room temperature is not glasslike but exhibits some remnants of crystalline behavior.

The electrical transport in the filled skutterudites is altered by the presence of the rattlers. Relative to the analogous unfilled compounds, the filled skutterudites exhibit larger effective masses and smaller mobilities. Good overall electrical transport is maintained as indicated by the large values of ZT at elevated temperatures. The high carrier concentrations in the filled skutterudites are due mostly to the fraction of the rare-earth sites that remain empty in samples prepared using equilibrium synthesis methods. A simple semiconductor transport model successfully reproduces most of the qualitative features of the resistivity and Seebeck data from these materials. By varying the extrinsic carrier concentration in the filled skutterudites, this model yields a maximum value for ZT of 1.4 at 1000 K, and a maximum ZT value of 0.3 at 300 K.

Above room temperature, there is very little difference in the electrical and thermal transport behavior between the La and Ce filled compounds. The low-temperature resistivity data from the Ce compounds are not accounted for by a simple transport model, but are characteristic of the effects of hybridization caused by the proximity of the Ce 4*f* level to the Fermi energy. An analysis of the magnetic susceptibility data indicates the presence of a crystalline electric field that splits the $J=5/2$ Hund's rule state of the Ce^{+3} ion into a ground state doublet and a quartet at an energy of 350 K. The magnetic susceptibility data suggest that the Ce valence is close to 3 over the entire temperature range.

ACKNOWLEDGMENTS

It is a pleasure to acknowledge useful discussions with G. D. Mahan. Research was sponsored in part by a Cooperative Research and Development Agreement with Marlow Industries, and in part by the Division of Materials Sciences, U. S. Department of Energy Contract No. DE-ACO5-96OR22464. Oak Ridge National Laboratory is managed by the Lockheed-Martin Energy Research Corporation.

¹G. A. Slack, *CRC Handbook of Thermoelectrics*, edited by D. M. Rowe (Chemical Rubber, Boca Raton FL, 1995), Chap. 34, p. 407.

²G. A. Slack, *Solid State Physics: Advances in Research and Applications*, edited by H. Ehrenreich, F. Seitz, and D. Turnbull (Academic, New York, 1979), Vol. 34, pp. 1–73.

³D. G. Cahill, S. K. Watson, and R. O. Pohl, *Phys. Rev. B* **46**, 6131 (1992).

⁴W. Jeitschko and D. J. Braun, *Acta Crystallogr., Sect. B: Struct. Crystallogr. Cryst. Chem.* **33**, 3401 (1977).

⁵D. J. Braun and W. Jeitschko, *J. Less-Common Met.* **72**, 147 (1980).

⁶D. J. Braun and W. Jeitschko, *J. Solid State Chem.* **32**, 357 (1980).

⁷D. J. Braun and W. Jeitschko, *J. Less-Common Met.* **76**, 33 (1980).

- ⁸G. A. Slack and V. G. Tsoukala, *J. Appl. Phys.* **76**, 1665 (1994).
- ⁹N. T. Stetson, S. M. Kauzlarich, and H. Hope, *J. Solid State Chem.* **91**, 140 (1991).
- ¹⁰L. E. DeLong and G. P. Meisner, *Solid State Commun.* **53**, 119 (1985).
- ¹¹D. M. Morelli and G. P. Meisner, *J. Appl. Phys.* **77**, 3777 (1995).
- ¹²G. P. Meisner, M. S. Torikachvili, K. N. Yang, M. B. Maple, and R. P. Guertin, *J. Appl. Phys.* **57**, 3073 (1985).
- ¹³M. E. Danebrock, C. B. H. Evers, and W. Jeitschko, *J. Phys. Chem. Solids* **57**, 381 (1996).
- ¹⁴G. P. Meisner, *Physica B & C* **108B**, 763 (1981).
- ¹⁵S. Zemi, D. Tranqui, P. Chaudouet, R. Madar, and J. P. Senateur, *J. Solid State Chem.* **65**, 1 (1986).
- ¹⁶I. Shirovani, T. Adachi, K. Tachi, S. Todo, K. Nozawa, T. Yagi, and M. Kinoshita, *J. Phys. Chem. Solids* **57**, 211 (1996).
- ¹⁷T. Caillat, A. Borshchevsky, and J. P. Fleurial, *Proceedings of the Eleventh International Conference on Thermoelectrics, Arlington, Texas, 1993*, edited by K. R. Rao (University of Texas Press, Arlington, Texas, 1993), pp. 98–102.
- ¹⁸J.-P. Fleurial, T. Caillat, and A. Borshchevsky (unpublished).
- ¹⁹J. W. Sharp, E. C. Jones, R. K. Williams, P. M. Martin, and B. C. Sales, *J. Appl. Phys.* **78**, 1013 (1995).
- ²⁰B. C. Sales, D. Mandrus, and R. K. Williams, *Science* **272**, 1325 (1996).
- ²¹A. Migliori, J. L. Sarrao, W. M. Visscher, T. M. Bell, M. Lei, Z. Fisk, and R. G. Leisure, *Physica B* **183**, 1 (1993).
- ²²B. C. Chakoumakos (private communication).
- ²³D. Mandrus, B. C. Sales, V. Keppens, B. C. Chakoumakos, P. Dai, L. A. Boatner, R. K. Williams, T. W. Darling, A. Migliori, M. B. Maple, D. A. Gajewski, and E. J. Freeman, *Proceedings of Thermoelectric Materials-New Directions and Approaches*, edited by T. M. Tritt, G. Mahan, H. B. Lyon, and M. G. Kanatzidis, *MRS Symposia Proceedings No. 478* (Material Research Society, Pittsburgh, PA, 1997), pp. 199–209.
- ²⁴C. Kittel, *Introduction to Solid State Physics* (Wiley, New York, 1968), p. 186.
- ²⁵J.-P. Fleurial, A. Borshchevsky, T. Caillat, D. T. Morelli, and G. P. Meisner, in *Proceedings of the Fifteenth International Conference on Thermoelectrics, Pasadena, CA* (IEEE, Piscataway, NJ, 1996), p. 91.
- ²⁶H. J. Goldsmid, *Electronic Refrigeration* (Pion Limited, London, 1986), pp. 29–63.
- ²⁷B. C. Sales (unpublished).
- ²⁸B. Chen, J. H. Xu, C. Uher, D. T. Morelli, G. P. Meisner, J. P. Fleurial, T. Caillat, and A. Borshchevsky, *Phys. Rev. B* **55**, 1476 (1997).
- ²⁹D. Singh and I. I. Mazin, *Phys. Rev. B* **56**, R1650 (1997).
- ³⁰B. C. Sales and R. Viswanathan, *J. Low Temp. Phys.* **23**, 449 (1976).
- ³¹K. R. Lea, M. J. K. Leask, and W. P. Wolf, *J. Phys. Chem. Solids* **23**, 289 (1962).
- ³²M. B. Maple, L. E. DeLong, and B. C. Sales, *Handbook on the Physics and Chemistry of Rare Earths*, edited by K. A. Gschneidner and L. Eyring (North-Holland, New York, 1978), Chap. 11.